Electronic Supplementary Material (ESI) for Nanoscale.
This journal is © The Royal Society of Chemistry 2020

Supplementary Information for

Charge carrier pairing can impart efficient reduction efficiency to core/shell quantum dots: Applications for chemical sensing

Marcell Pálmai,[a] Eunbyoel Kim,[a] Vincent Schnee[b] and Preston T. Snee[a]*

[a]Department of Chemistry, University of Illinois at Chicago, 845 W. Taylor Street, Chicago, Illinois 60607-7061, United States

[b]US Army CCDC C5ISR Night Vision and Electronic Sensors Directorate, United States Army, Fort Belvoir, VA, 22060-5806 United States

*E-mail: sneep@uic.edu

Index	*Page*
Chemicals and Instrumentation	S2
Fig. S1 TEM images of thick shell CdZnS/ZnS QDs.	S3
Fig. S2 Titration of CdZnS and CdZnS/ZnS QDs and fits to a modified isotherm model.	S3
Fig. S3 Stern-Volmer analyses of CdZnS QDs as a function of quantum yield.	S4
Fig. S4 Time resolved emission of CdZnS and CdZnS/ZnS QDs.	S5
Table S1 Parameters from time resolved emission data.	S5
Fig. S5 Natural Transition Orbitals for various cluster-TNT model systems.	S6
Table S2 Parameters for effective mass modeling.	S7
Fig. S6 PES of CdSe/CdS and CdZnS/ZnS QDs.	S8
Fig. S7 Hole probability of CdSe/CdS as a function of shell thickness.	S9
Fig. S8 Hole probability of CdZnS/ZnS as a function of shell thickness.	S10
Fig. S9 Hole probability of CdS/ZnS as a function of core radius.	S11
References	S11

Chemicals

Dodecylamine (98%), zinc oxide (ZnO, nanopowder), diethyl zinc (Et_2Zn, 95%), hexamethyldisilathiane ($(TMS)_2S$, 95%), n-hexane (>98.5%), isopropanol (>99.5%), methanol (99.9%), 1-octadecene (ODE, 90%), oleic acid (90%), oleylamine (90%), sulfur (99.98%), and 2,4,6-trinitrotoluene (TNT) were purchased from Sigma-Aldrich. Cadmium oxide brown (CdO, ≥99.0%) was purchased from Fluka. Trioctylphosphine (TOP, 97%) was obtained from Strem. Et_2Zn and $(TMS)_2S$ were stored at -30 ºC in an inert N_2 atmosphere glove box. Oleic acid was recrystallized prior to use. Oleylamine was purified by vacuum distillation over KOH and was stored under inert atmosphere. Cadmium oleate solutions for overcoating were prepared by mixing CdO and 2.2× excess oleic acid (by mole) in ODE and heating to 270 °C until optical clarity was realized, typically ~45 min. All other reagents were used without further purification.

Instrumentation

Morphological investigations of the different QD samples were carried out on a JEOL JEM-3010 transmission electron microscope operating at 300 kV. Diluted samples were dropped and dried on carbon coated gold grids. Fluorescence spectra were recorded using a HORIBA FluoroMax-4 spectrofluorimeter. UV/Vis spectroscopy measurements were performed with a Varian Cary 300 Bio spectrophotometer. Emission lifetimes were measured using a homebuilt system composed of an SRS NL100 N_2 laser excitation source, the output of which was resolved with a Jarrell Ash monochromator coupled to an Applied Physics photomultiplier tube (PMT) detector. Time resolved data was obtained by coupling the PMT output to a 1GHz Tektronix TDS5104B oscilloscope as triggered by a photodiode.

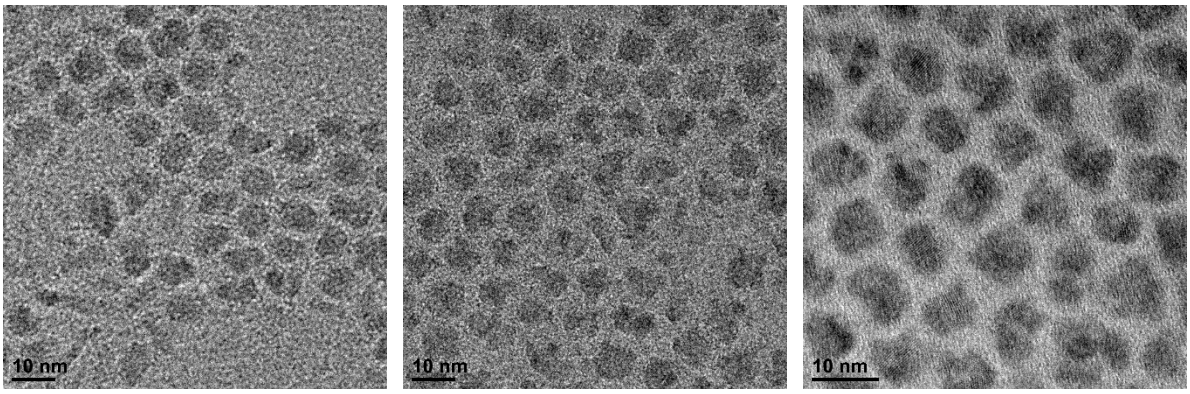

Fig. S1 TEM analysis of thick shell CdZnS/ZnS QDs reveals some heterogeneity in the sample population.

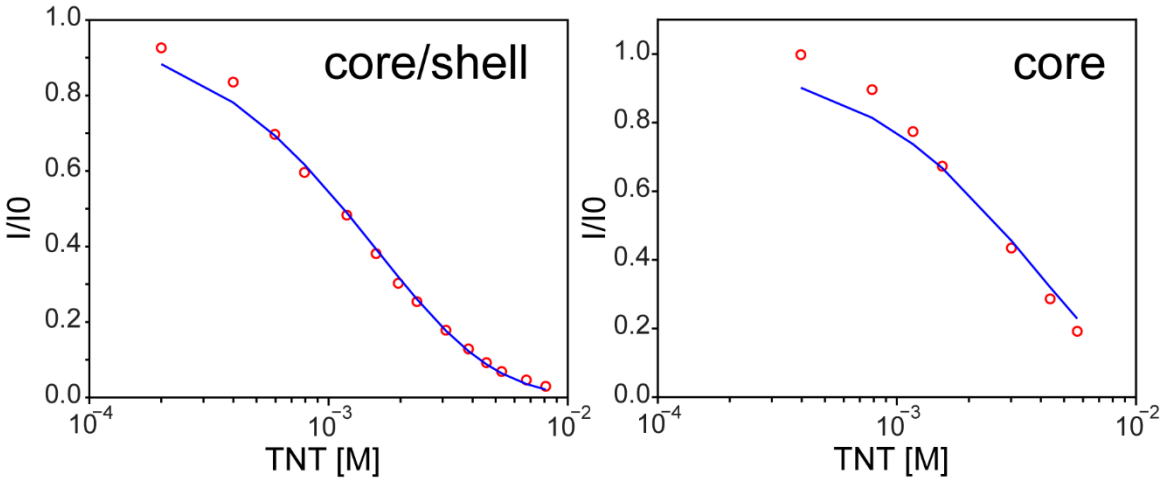

Fig. S2 Fluorescence response of CdZnS and thin shell CdZnS/ZnS QDs to TNT exposure over a wide range was analyzed via the method of Morris-Cohen et al. Data fitting used [QD] ~1×10^{-7} M and was corrected for dilution; the total number of TNT sites was estimated as N=114 for core and N=142 for the core/shell using an area of 0.256 nm^2 for the TNT molecule (see ref.1). The fittings yield unphysically low values for the association constant (K_A= 42 M^{-1} and 2 M^{-1} for the core/shell and core, respectively), an artefact likely due to the lack of unit efficient TNT quenching. The core also can experience some brightening due to low levels of TNT exposure, which may be due to photobrightening during the experiment. Regardless, the best fits to the data reveal that the K_A of the core/shell is higher than the core, which is consistent with DFT results discussed in the main text.

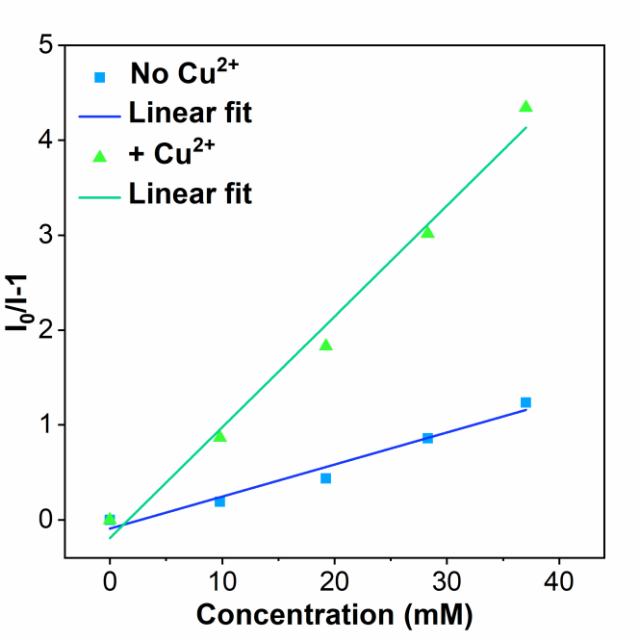

Fig. S3 The effect of finite quantum yield on Stern-Volmer constants was measured on CdZnS QDs. A sample was split into two fractions, whereby one was used as-prepared while the other was quenched by copper to reduce the CdZnS dots' quantum yield by ~50%. Both samples were then titrated with equivalent concentrations of nitrobenzene. As can be seen, a lower emission efficiency is related to a higher Stern-Volmer constant.

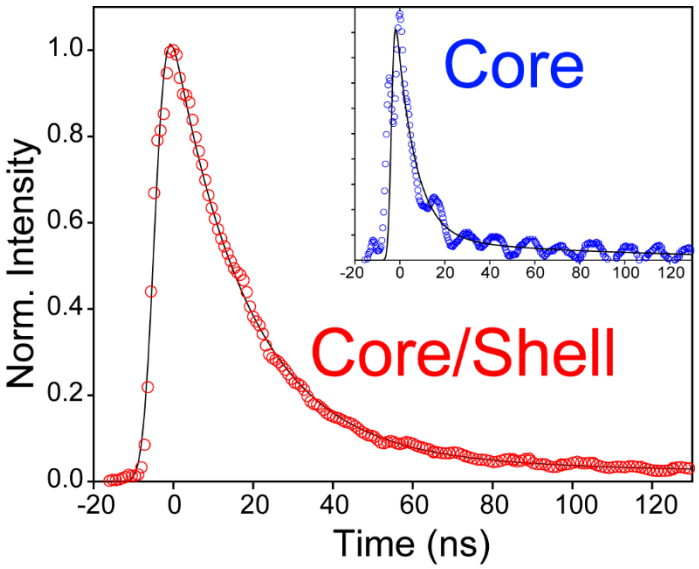

Fig. S4 Time resolved emission of core CdZnS and core/shell CdZnS/ZnS QDs reveals a longer lifetime in the latter, which in turn is correlated to an enhanced Stern-Volmer constant. Data were fit to the equation: $I(t) = A_1 e^{-t/\tau_1} + A_2 e^{-t/\tau_2}$.

Table S1 Time resolved CdZnS and CdZnS/ZnS emission parameters. Fits were convolved with an instrument response of 2.9 ns. Errors were estimated using the variance-covariance method.

Sample	A_1	τ_1 (ns)	A_2	τ_2 (ns)
CdZnS	0.92 ± 0.08	8 ± 2	0.08 ± 0.08	100 ± 800
CdZnS/ZnS	0.957 ± 0.002	18.68 ± 0.08	0.043 ± 0.002	200 ± 10

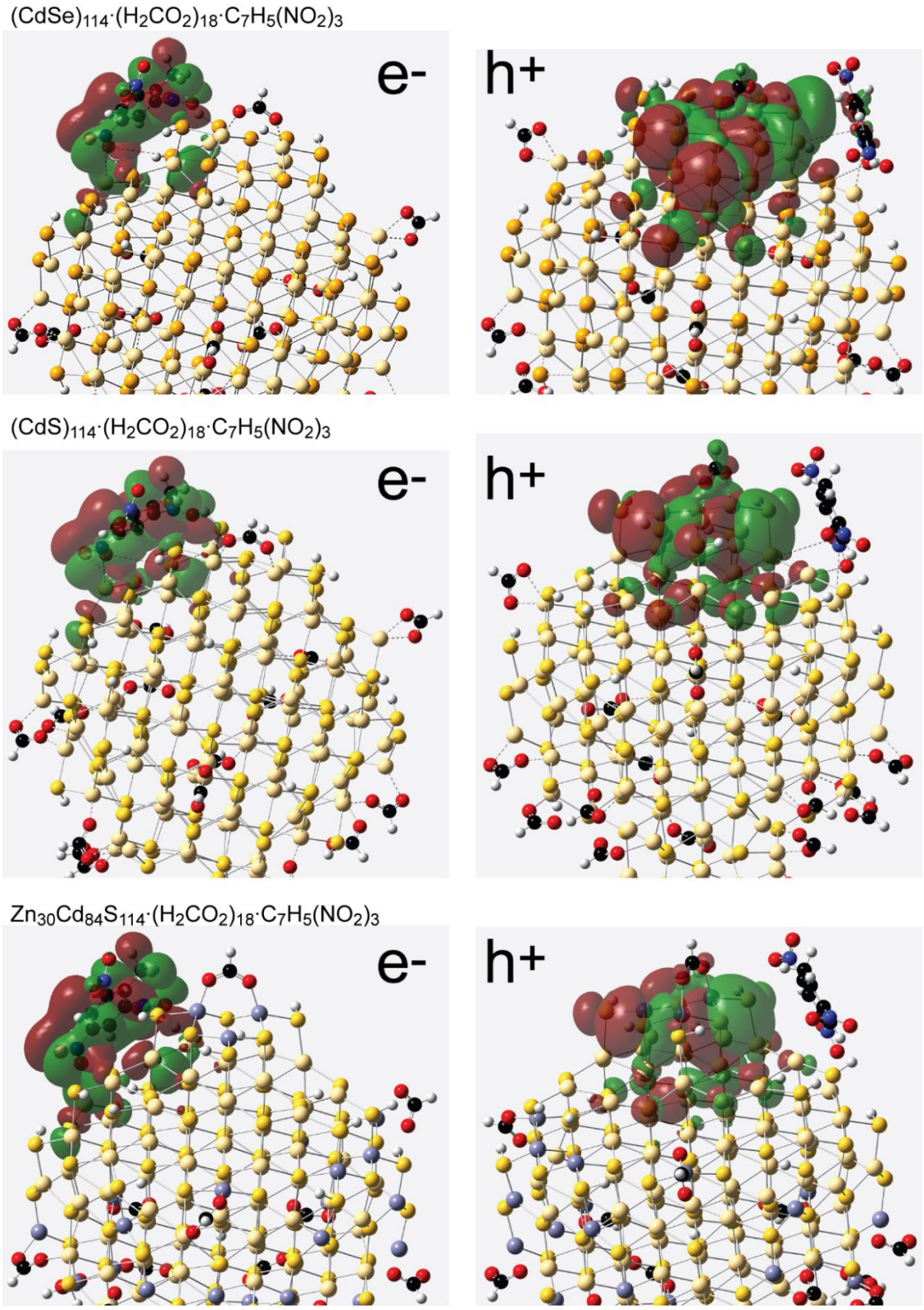

Fig. S5 Natural Transition orbitals from TDDFT calculations of various quantum dot – TNT models reveal reduction of the substrate for all systems under consideration.

Potential energy surface for effective mass calculations

The hole wavefunctions and probability densities were solved using an effective mass (i.e. particle-in-a-sphere) model, with reduced hole masses and dielectric constants from the literature with and without an exterior electron that is placed 3Å from the outside of the shell. The sphere center is (0,0,0). The CdSe/CdS and CdZnS/ZnS models have 2.2 nm and 3.0 nm core radii, respectively, as determined from TEM characterizations from real samples. The CdZnS core was modeled as an alloy with a parabolic compositional change from pure CdS to ZnS. Several shell thicknesses were examined with a monolayer of shell defined as having a 3.5 Å thickness. The exterior is composed of ligands with an effective mass of m_0 and a potential energy (i.e. barrier) of 10 eV.
The potential from an exterior electron is based on classical electrostatics, whereby the Coulomb operator is expanded in a Taylor series of Legendre polynomials $P_l(\cos(\theta))$. The $\cos(\theta)$ is the angle from the electron, sphere center, and a point on the 3D 256^3 grid. The potential at all grid points must be calculated which is time-consuming. The distance from the center to the exterior electron is d, which is simply assumed to reside along the x-axis. The electrostatic contribution to the potential energy inside the nanomaterial is:

$$\frac{q}{4\pi\epsilon_{sc}d}\sum_{l=0}^{\infty} P_l(\cos(\theta)) \cdot \left(\frac{r}{d}\right)^l \cdot \frac{2l+1}{\frac{\epsilon_0}{\epsilon_{sc}} \cdot l + \frac{\epsilon_0}{\epsilon_{sc}} + l}$$

The potential energy between the exterior of the shell and the electron is:

$$\frac{q}{4\pi\epsilon_{sc}d}\sum_{l=0}^{\infty} P_l(\cos(\theta)) \cdot \left(\left(\frac{r}{d}\right)^l + \frac{\frac{\epsilon_0}{\epsilon_{sc}} \cdot l - l}{\frac{\epsilon_0}{\epsilon_{sc}} \cdot l + \frac{\epsilon_0}{\epsilon_{sc}} + l} \cdot \left(\frac{a}{d}\right)^l \cdot \left(\frac{a}{r}\right)^{l+1}\right)$$

And at larger radial distances than the electron (i.e. r>d):

$$\frac{q}{4\pi\epsilon_{sc}d}\sum_{l=0}^{\infty} P_l(\cos(\theta)) \cdot \left(\frac{d}{r}\right)^{l+1} \cdot \left(1 + \left(\frac{a}{d}\right)^{2l+1} \frac{\frac{\epsilon_0}{\epsilon_{sc}} \cdot l - l}{\frac{\epsilon_0}{\epsilon_{sc}} \cdot l + \frac{\epsilon_0}{\epsilon_{sc}} + l}\right)$$

Table S2 List of Material Parameter for Calculations.

Material	band gap (eV)	Electron barrier (eV)	Hole Barrier (eV)	e^- mass	h^+ mass
CdSe	1.75	-	-	0.13	0.5
CdS	N/A	0.24	0.42	0.21	0.7

Material	band gap (eV)	Electron barrier (eV)	Hole Barrier (eV)	e^- mass	h^+ mass
CdS	2.24	-	-	0.21	0.70
ZnS	N/A	0.94	0.18	0.34	1.75

Parameters from references 2 and 3. Note that only holes were modeled. Dielectric constants were: CdSe, $\epsilon_{sc} = 6.2$; CdZnS, $\epsilon_{sc} = 8.9$; ZnS, $\epsilon_{sc} = 8.9$, ligands, $\epsilon_{sc} = 1.0$. The formula above applies only to a homogeneous dielectric sphere, and not a core/shell with a discontinuity in the dielectric constant. As a result, the CdSe/CdS QDs used a homogeneous effective dielectric constant derived according to reference 4.

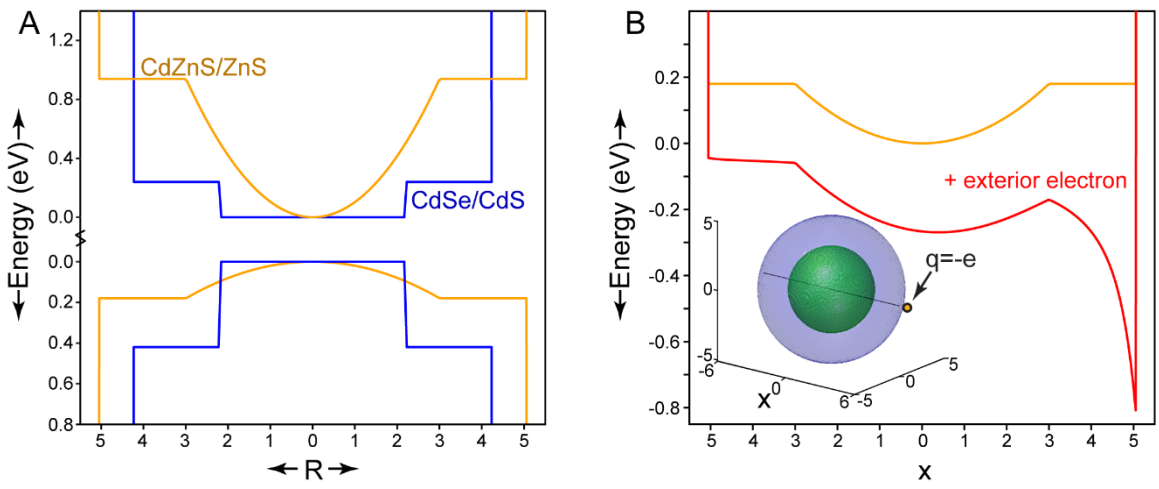

Fig. S6 (A) Electron and hole potential energy surfaces of CdSe/CdS and CdZnS/ZnS with core radii of 2.2 and 3.0 nm, respectively. The shell thickness here is for 6 monolayers. For computational convenience, the hole states are solved with the potential surface "upright", imparting positive energies that are added to the bandgap to simulate quantum confinement energy. An example is shown in (B), where the effect on the PES of the external electron is shown along a center line of the nanomaterial.

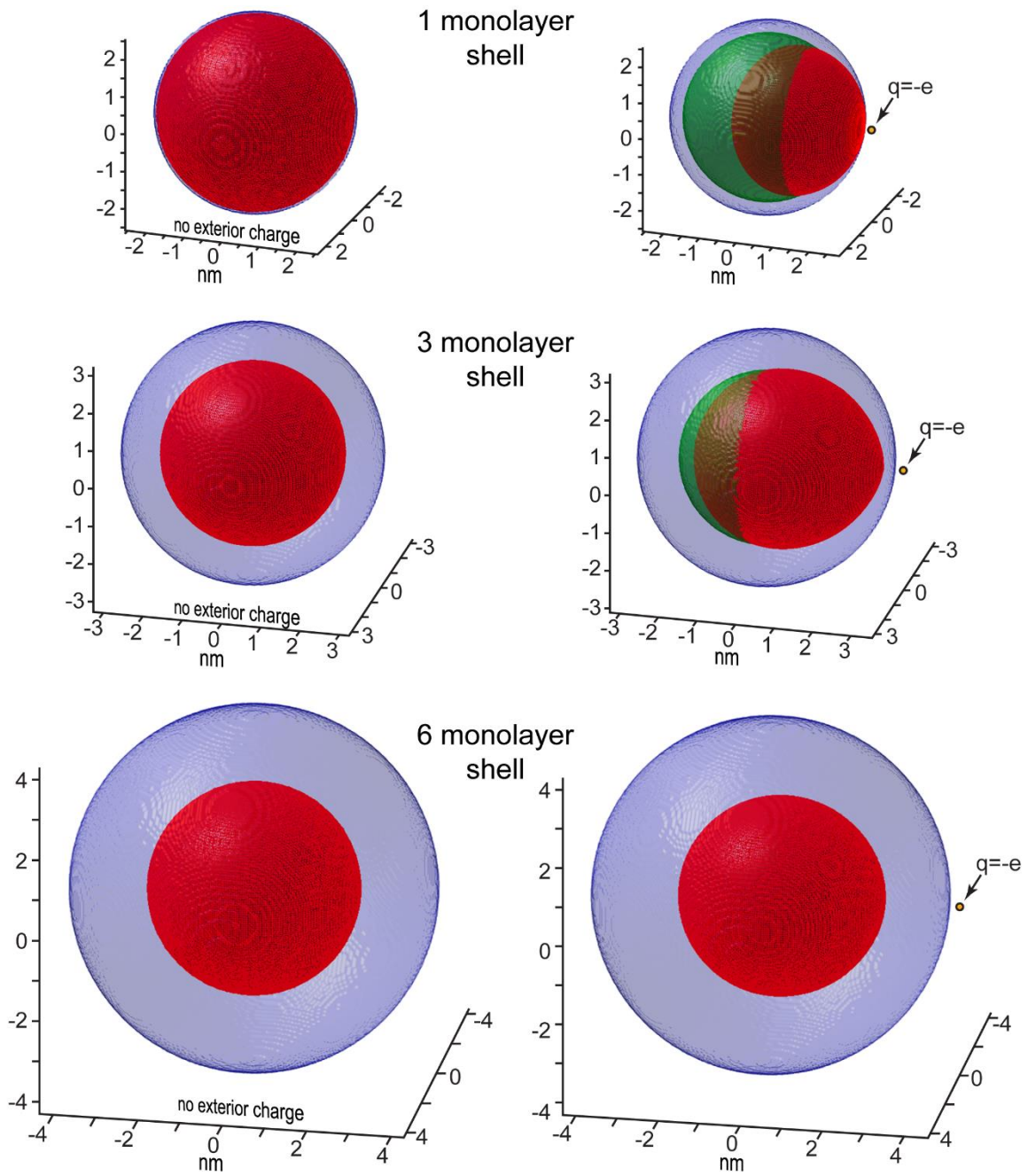

Fig. S7 95% probability isosurfaces of core/shell CdSe/CdS QD holes as a function of shell thickness. On the left, holes (red) are localized and overlap the 2.2 nm radius core boundary (green); the shell surface is blue. On the right, an external negative charge polarizes the hole towards the exterior. An isosurface probability density of 85% was used for the 6 mololayer case in the main text (Fig. 5) because, as can be seen here, the hole state overlaps the core boundary which makes interpretation of that data more difficult.

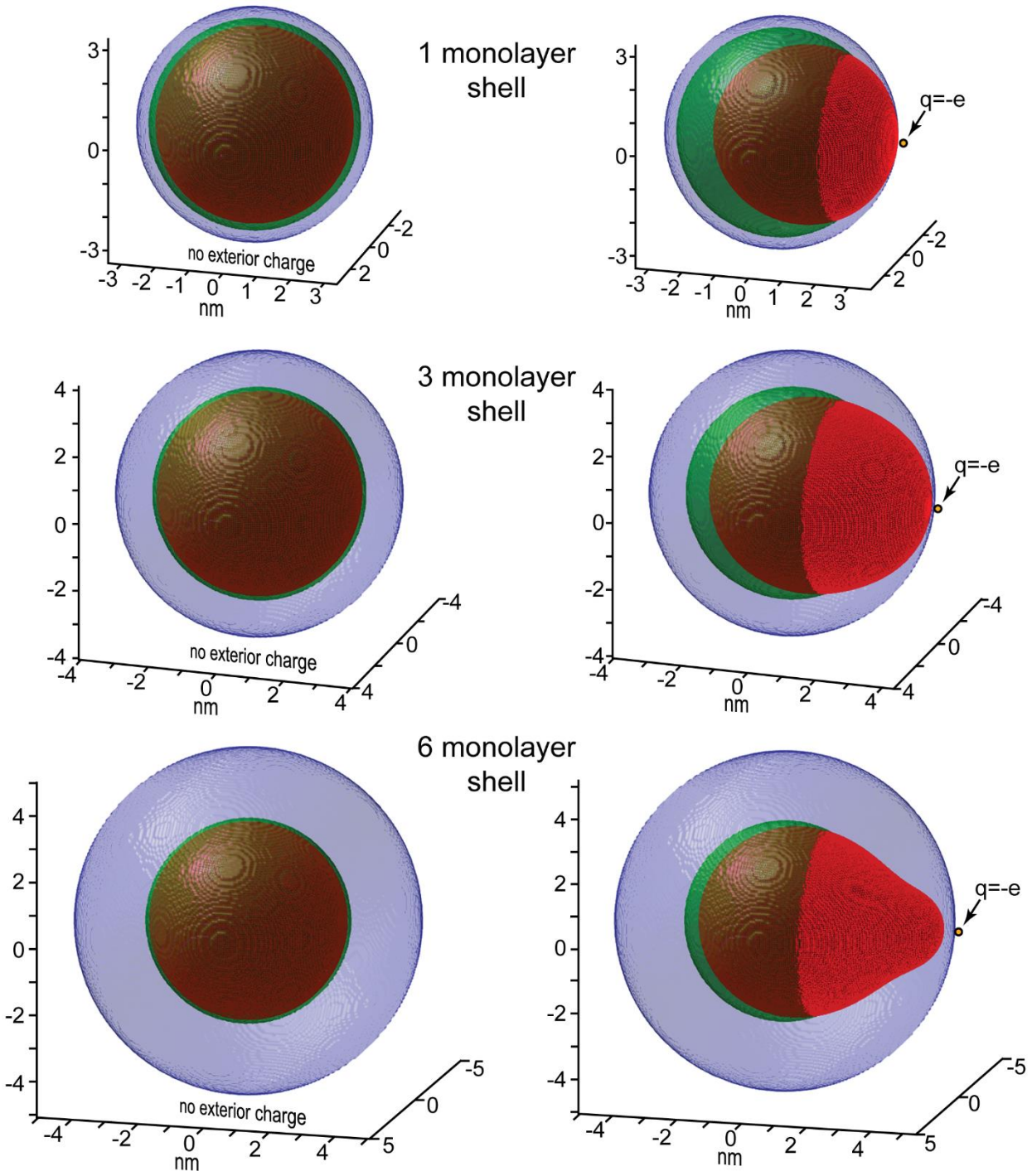

Fig. S8 95% probability isosurfaces of core/shell CdZnS/ZnS QD holes as a function of shell thickness. On the left, holes (red) are localized and overlap the 3.0 nm radius core boundary (green); the shell surface is blue. On the right, an external negative charge polarizes the hole towards the exterior.

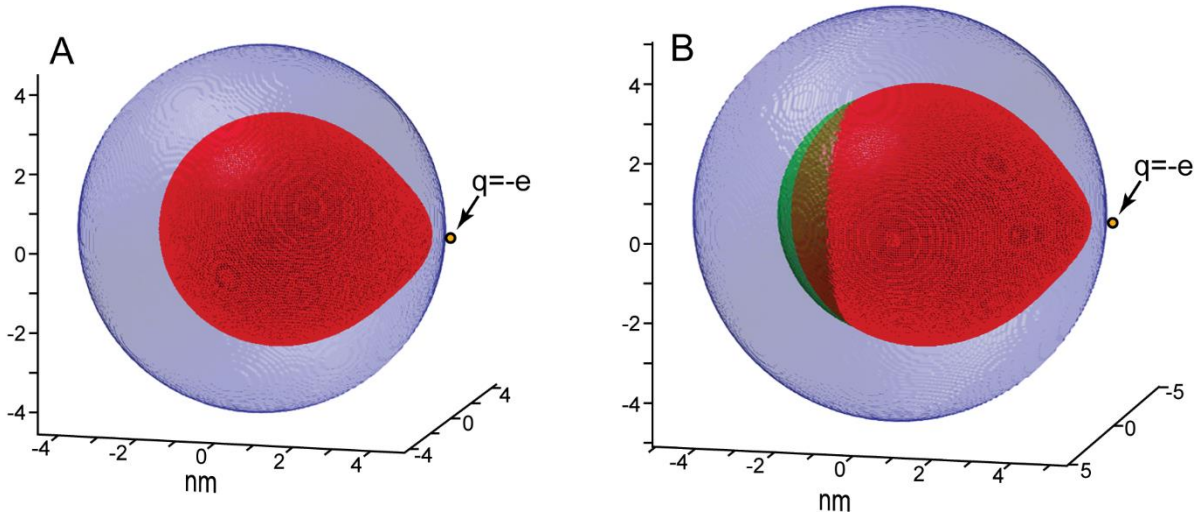

Fig. S9 95% probability isosurfaces of core/shell CdS/ZnS holes as a function of core radius reveal that the alloying of CdZnS cores is not responsible for hole localization near the surface of CdZnS/ZnS nanoparticles (Fig. S8). Holes (red) are localized and overlap the core boundary (green); the shell surface is blue. An external negative charge polarizes the hole towards the exterior. (A) Data from a 2.45 nm radius CdS core that has the same hole confinement energy as a 3.0 nm radius CdZnS nanoparticle. (B) The same for a 3.0 nm radius CdS core particle.

References

1 A. J. Morris-Cohen, M. T. Frederick, L. C. Cass and E. A. Weiss, *J. Am. Chem. Soc.*, 2011, **133**, 10146–10154.

2 R. Toufanian, A. Piryatinski, A. H. Mahler, R. Iyer, J. A. Hollingsworth and A. M. Dennis, *Front. Chem.*, , DOI:10.3389/fchem.2018.00567.

3 U. Soni, A. Pal, S. Singh, M. Mittal, S. Yadav, R. Elangovan and S. Sapra, *ACS Nano*, 2014, **8**, 113–123.

4 L. F. Chen, C. K. Ong, B. T. G. Tan and C. R. Deng, *Journal of Materials Science*, 1998, **33**, 5891–5894.